

# Diaphragm-type Acoustic Sensor Based on Sputtered Piezoelectric Thin Film

Atul Garg and K. Rajanna\*

Department of Instrumentation, Indian Institute of Science  
Bangalore 560012, India

(Received August 25, 2004; accepted September 13, 2005 )

**Key words:** acoustic sensor, diaphragm, piezoelectric thin film, sound pressure level, frequency response

In this paper, we report the development of a low-cost acoustic sensor using piezoelectric ZnO thin film deposited onto a thin stainless-steel diaphragm. The details of the diaphragm and the mechanical assembly of the sensor are given. Reactive magnetron sputtering has been used for the preparation of piezoelectric ZnO film. Studies on the characterization of the ZnO films for the confirmation of their piezoelectric behavior are included. Observations on the performance of the acoustic sensor are presented, which include frequency response characteristics, sensitivity and linearity. In comparison with general acoustic sensors, our acoustic sensor is attractive in view of its low cost, lower weight and simpler fabrication methods.

## 1. Introduction

Acoustic sensors are an important link in sound reproduction and communication systems. In general, any sound-transmitting system contains two fundamental elements: an instrument for converting sound energy into electrical energy, and an instrument for converting electrical signals into acoustical energy.<sup>(1,2)</sup> These instruments are termed as electroacoustic transducers. Acoustic sensors find wide application in areas such as consumer products (telephone circuits, speech amplifiers, tape recorders and hearing aids), and space, medical and industrial equipments.<sup>(3,4)</sup> The human ear is a natural acoustic transducer with tolerance for wide amplitude variations. However, it either fails or becomes impossible to use in hazardous environments, because of radiation, and in remote areas. Therefore, there is increasing interest in developing acoustic sensors which can be used to sense high-intensity sounds and are suitable for use under adverse environmental conditions.

---

\*Corresponding author, e-mail address: kraj@isu.iisc.ernet.in

In this paper, we report on the development and performance study of a low-cost acoustic sensor with a piezoelectric thin film on a diaphragm made of stainless steel (SS-304L), which is suitable for high-intensity sound (up to 150 dB) in hazardous and radiation-exposed environments.

## 2. Experimental

In our work on the development of acoustic sensor, we have used piezoelectric thin film to convert an acoustic input signal into a proportional electrical output. There are several possible advantages of a piezoelectric transducer, which include ease of processing and robust design.<sup>(5-7)</sup> Also, piezoelectric acoustic sensors, which do not involve an air gap, are known to have more robust fabrication processes than capacitive acoustic sensors.<sup>(8)</sup>

### 2.1 Fabrication of mechanical assembly for sensor

Figure 1 shows a schematic of the mechanical assembly designed for the sensor in our present work. The mechanical assembly of the sensor, with the necessary apparatus for fixing the diaphragm in place, is made of perspex, which is transparent, electrically insulating, cheap, light and easily machinable. The diaphragm, the primary sensing element of the acoustic sensor, is made of stainless steel 304L (SS-304L, a special grade of stainless steel). It has many properties ideal for its use as a sensing element in the acoustic sensor. Some of the important features of SS-304L are the following.

- It has a high mechanical strength, withstands fatigue and creep and is resistant to environmental corrosion.
- It can be continuously exposed to high temperatures up to  $\sim 800^{\circ}\text{C}$  without appreciable scaling.
- In addition, it is known to exhibit a high linearity, a low hysteresis and a good repeatability with respect to its elastic behavior.

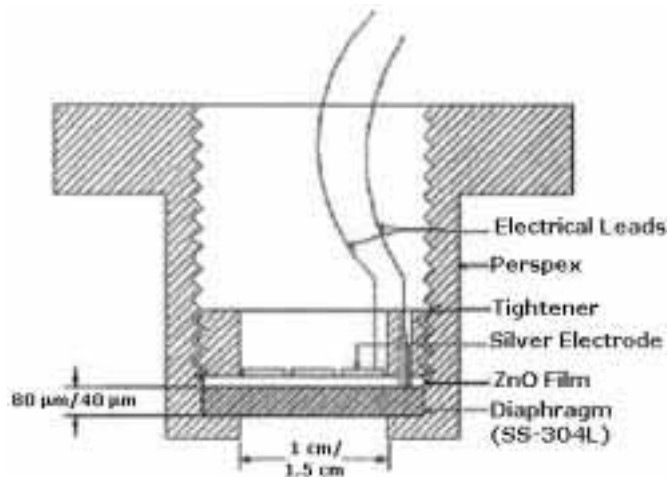


Fig. 1. Schematic view of cross section of acoustic sensor.

## 2.2 *Choosing suitable piezoelectric material and its preparation in thin-film form*

Piezoelectric material plays an important role in the development of acoustic sensors. Over the last decade, many researchers have reported the useful characteristics of piezofilms prepared using different growth methods for different applications. We have used ZnO piezoelectric thin film as the sensing film in our acoustic sensor because of its better piezoelectric coupling (compared with other nonceramic materials) and the greater stability of its hexagonal phase.<sup>(9)</sup> Another advantage of ZnO is the ease of depositing a high-quality thin film exhibiting piezoelectric properties. ZnO has proven to be a compositionally simple piezoelectric material, which can be sputtered as a high-quality film on a variety of conducting, semiconducting and insulating substrates. It does not require any pooling, unlike bulk PZT materials, for it to exhibit piezoelectric properties.

The thin films of ZnO can be prepared using various deposition techniques such as vacuum evaporation, reactive evaporation, spray pyrolysis, spray-chemical vapor deposition, chemical vapor deposition, metalorganic chemical vapor deposition, sol-gel process, laser deposition, laser molecular beam epitaxy, plasma assisted molecular epitaxy, ion beam sputtering, AC sputtering, DC sputtering, DC magnetron sputtering, and RF magnetron sputtering. Among these methods, DC magnetron sputtering has received much attention for the preparation of transparent oxide films using a metal target because high deposition rates can be achieved on large-area substrates and the composition of the films can easily be controlled. In our work, we have prepared piezoelectric ZnO thin films by DC reactive magnetron sputtering.

The depositions of ZnO films were carried out both at room temperature as well as at higher substrate temperatures. For in-situ annealing, substrate-heating equipment including an iron-box heating element was used. A circular Zn target of 99.9% purity with a diameter of 75 mm and a thickness of 3 mm was employed. Before loading the substrates in the chamber for deposition, they were thoroughly cleaned with soap water to remove any grease, ultrasonically cleaned to remove any dust particles trapped at the surface, and rinsed with organic solvent to remove any remaining soap, followed by removing the dust particles at the final stage (just before closing the chamber) using a pipette-like blower. First, the chamber was evacuated to an ultimate vacuum of  $\sim 1 \times 10^{-5}$  mbar. By introducing liquid nitrogen into the trap located between the chamber and the diffusion pump, the vacuum in the chamber could be improved to  $6 \times 10^{-6}$  mbar. Initially, reactive oxygen gas (99.9% pure) was supplied and subsequently, inert gas argon (99.9% pure) was introduced. Depositions were carried out at different temperatures and different pressure ratios between argon and oxygen. The various parameters optimized for the deposition of good piezoelectric films are shown in Table 1.

## 2.3 *Characterization of piezoelectric ZnO thin film*

Before using the ZnO film in an acoustic sensor, deposited films were characterized by different methods to confirm their piezoelectric behavior. A brief description of these methods is given below.

Many direct and indirect methods exist for evaluating the piezoelectric behavior of deposited ZnO thin films.<sup>(10)</sup> In our work, we have used X-ray diffraction (XRD) for

Table 1  
Various deposition parameters optimized for deposition of ZnO thin films.

Base pressure	$6 \times 10^{-6}$ mbar
Working pressure	$1 \times 10^{-3}$ mbar
O <sub>2</sub> : Ar	3.5 : 6.5
Target-substrate distance	6.5 cm
Substrate temperature	200°C
Presputtering time	15 min
Current density	4.5393 mA/ cm <sup>2</sup>
Deposition rate	120 Å/ min

observing c-axis orientation and spectrophotometry for optical properties, as indirect methods, and a cantilever technique for observing the dynamic response, as a direct method. Figure 2 shows the XRD patterns of films deposited at 100°C and 200°C. The corresponding data obtained from the analysis of XRD patterns are given in Table 2. It has been observed that the increase in substrate temperature helps to relieve stress in the deposited films. The degree of c-axis orientation improved with temperature. The grain sizes achieved are close to the reported values.<sup>(11)</sup> Higher substrate temperatures might have increased the degree of c-axis orientation, as well as the grain size, still further, but larger grain size is not always desirable. As the grain size increases, the resulting surface becomes rougher, which is unfavorable for device applications.

Films were also deposited onto quartz substrates for the purpose of studying their optical properties. The transmission spectra of the films were recorded using an M/s Hitachi spectrophotometer (Model no. 330). Spectra were taken in the range of 300 nm to 1300 nm. The zinc oxide single crystal is a clear transparent material. High-acoustical-quality ZnO films are often described in terms of optical clarity. Good zinc oxide films are clear, while poor-quality films have a hazy or milky appearance.<sup>(12)</sup> Apart from the possibility of a stoichiometric imbalance of zinc and oxygen, which would cause discoloration, the milky appearance results from surface roughness. The refractive index of the film depends on the film orientation. Consequently, optical attenuation is also intimately related to refractive index. The transmission spectra obtained were analyzed using the Swanpoel technique. Data obtained from the analysis of the transmission spectra of the films deposited at various oxygen partial pressures and temperatures are given in Table 3. Film deposited with an oxygen to argon ratio of 3.5:65 at a substrate temperature of 200°C showed a band gap of 3.39 eV, which is close to the ideal value. This is supported by the high degree of c-axis orientation of the film deposited under the same conditions, as shown in Fig. 2. However, we have also adopted a direct method, namely, a cantilever technique, for the confirmation of piezoelectric properties of the ZnO thin films prepared. Films were tested by deflecting the cantilever not only upward, but also in the downward direction.

After the confirmation of the piezoelectric behavior of ZnO film and the optimization of the deposition process parameters, ZnO film was deposited onto the polished circular SS- 304L diaphragms. Subsequently, a silver electrode was deposited onto ZnO thin film, resulting in the formation of the metal-insulator-metal (MIM) configuration. This MIM configured diaphragm was firmly clamped circumferentially using a mechanical assembly

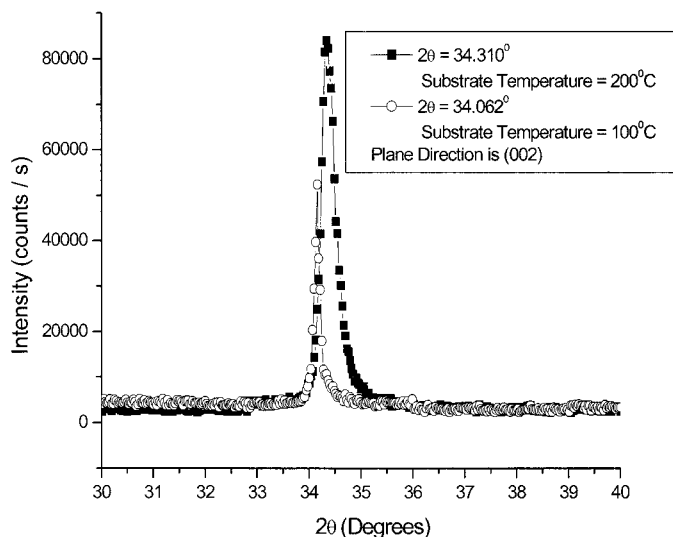


Fig. 2. XRD pattern of ZnO films deposited on stainless-steel substrate maintained at different temperatures.

Table 2

XRD data for ZnO films deposited on stainless-steel substrates maintained at different temperatures.

Temperature (°C)	$2\theta$	FWHM	d-spacing (Å)	Grain size (Å)
100	34.062°	0.45619°	2.6289	210.23
200	34.310°	0.41087°	2.61054	234.11

Table 3

Data on optical behavior of ZnO thin films deposited with different oxygen partial pressures and substrate temperatures.

O <sub>2</sub> : Ar	Temperature (°C)	Transmission (%)	Band gap (eV)
3.5 : 6.5	200	90	3.399
2.5 : 7.5	200	91	3.4676
2.5 : 7.5	150	88	3.4812

(Fig. 1). When the diaphragm is subjected to acoustic pressure, it becomes stressed, causing charge formation across the MIM configuration. To improve the sensitivity of the acoustic sensor, the top electrode was patterned (details given in § 3.1). Note that segmenting the electrode enhances sensitivity by selecting a smaller area of a higher strain rather than a larger area that includes a lower strain region.<sup>(13)</sup> The necessary stress and strain distribution analysis of the diaphragm was performed using Ansys simulation software.

## 2.4 Modeling and simulation

Prior to the development of the acoustic sensor, we analyzed various parameters, namely, sensitivity, displacement at the center of the diaphragm, and stress and strain generated in the diaphragm due to loading. The small-deflection theory is used to analyze parameters using Ansys simulation software. The small deflection theory includes the following assumptions.

- The maximum deflection due to applied load is small (i.e., not more than 30% of the thickness of the plate).
- The plate or diaphragm is flat and of uniform thickness; all forces, loads and reactions are applied normally to the plane of the plate.
- The plate is not stressed beyond the elastic limit and the deflection is mainly due to bending. Therefore, the median plane of the plate endures no tensile stress.

When a uniform force is applied onto the rigidly clamped diaphragm, the center of the diaphragm becomes more displaced compared with the other parts of the diaphragm. Therefore, to ensure a small deflection region, displacements at the center of the diaphragm are calculated (using harmonic analysis with Ansys) for diaphragms applied with a uniform pressure. A typical displacement for different nodes of the diaphragm (thickness 40  $\mu\text{m}$ , diameter 1 cm) is shown in Fig. 3.

In addition to the above, circular diaphragms of different sizes are modeled in ANSYS and analyzed for their distributions of strain and stress due to a uniform applied pressure. As the diaphragm is subjected to pressure, it becomes stressed and hence exhibits strain. The radial strain decreases rapidly as the radius increases, becomes negative, and then becomes twice the center strain at the edge. The tangential strain decreases from the center value to zero around the periphery of the diaphragm. It is shown in Fig. 4 that the diaphragm is subjected to compressive stress around the periphery and tensile stress at the central region of the diaphragm. However, the stress experienced near the periphery is

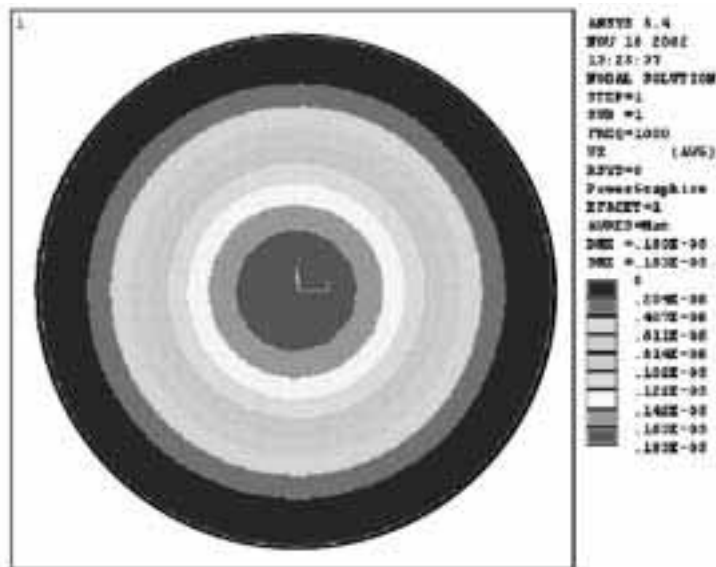


Fig. 3. Typical displacement distribution for diaphragm (thickness 40  $\mu\text{m}$ , diameter 1 cm).

greater in magnitude than the stress experienced at the center.

It is evident from the above results that the stress arising in the diaphragm reaches maximum around the periphery. Therefore, we have chosen an area closer to the periphery where stress is high and which covers enough of the region of the ZnO film for the deposition of the top electrode. A margin of 0.5 mm from the periphery is left to avoid damage likely to be caused by improper clamping. Keeping these aspects in mind, appropriate precision mechanical masks were designed and then fabricated by chemical etching.

### 3. Performance Study, Results and Discussion

A number of different measurements are required to determine the performance of an acoustic sensor. The most important characteristics which reflect the performance of an acoustic sensor are frequency response characteristics, linearity, sensitivity and directional characteristics.

A detailed study of the acoustic sensor performance is carried out using a calibration facility. A block diagram of the calibration setup used is shown in Fig. 5. It includes an acoustic calibrator, which is used to generate sound of different frequencies at different pressure levels. The acoustic calibrator has an opening where the sensor to be calibrated is mounted using a coupler to avoid any leakage of the sound generated by the acoustic

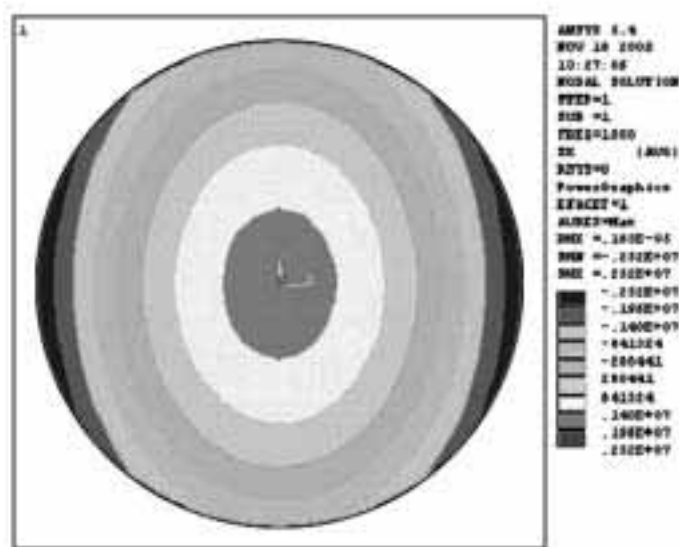


Fig. 4. Typical stress distribution for diaphragm (thickness 40  $\mu\text{m}$ , diameter 1 cm).

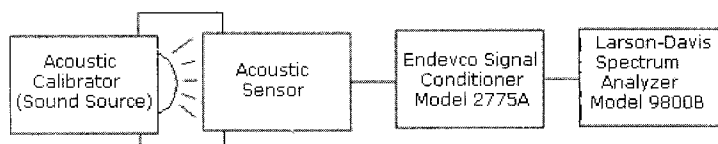


Fig. 5. Block diagram of calibration setup used for studying performance of acoustic sensor.

calibrator. The acoustic calibrator output is transmitted to an Endevco charge amplifier through a microdot cable. Charge-mode piezoelectric transducers require charge amplifiers to convert their output to useful voltage levels. To observe the response of the acoustic sensor at various acoustic pressure levels, the charge amplifier output is sent to a spectrum analyzer.

### 3.1 Frequency response characteristics

The acoustic sensor's frequency response curve illustrates the sensor's ability to transform acoustic energy into electrical signals.<sup>(14)</sup> The frequency response of an acoustic sensor is a measure of the consistency with which it translates a given sound pressure level into a proportional electrical signal at different frequencies. In our present study, the response of our acoustic sensor was recorded by varying the frequencies of the input signal. The data recorded are shown in Fig. 6. As mentioned above (in § 2.3), the response of the sensor can be improved by patterning the electrode deposited onto the ZnO thin film. The patterning of the electrode creates a minimum area with maximum stress, improving the sensor's response. The deposition of the silver electrode with the optimized area was carried out on the ZnO thin film using precision mechanical masks, and subsequently, frequency response characteristics were obtained. A schematic of the mechanical mask used is shown in Fig. 7(A). A schematic of the stainless-steel diaphragm with the ZnO thin film and patterned silver electrodes and its cross-sectional view are shown in Figs. 7(B) and 7(C), respectively. The corresponding recorded data are shown in Fig. 8. It is clear from Figs. 6 and 8 that the patterning of the silver electrode results in the improvement of the sensor's response by more than 35%.

### 3.2 Sensitivity and linearity

Sensitivity expresses the acoustic sensor's ability to convert acoustic pressure to a proportional electric voltage.<sup>(15)</sup> The sensitivity indicates the voltage a microphone produces at a certain sound pressure level (SPL). The sensitivity of our acoustic sensor is found to be around 5 mV at SPL of 140 dB with 1 kHz as forcing frequency. The linearity of the acoustic sensor is examined by plotting acoustic sensitivity as a function of SPL at a fixed frequency.<sup>(16)</sup> Figure 9 illustrates the unamplified linear response of the acoustic

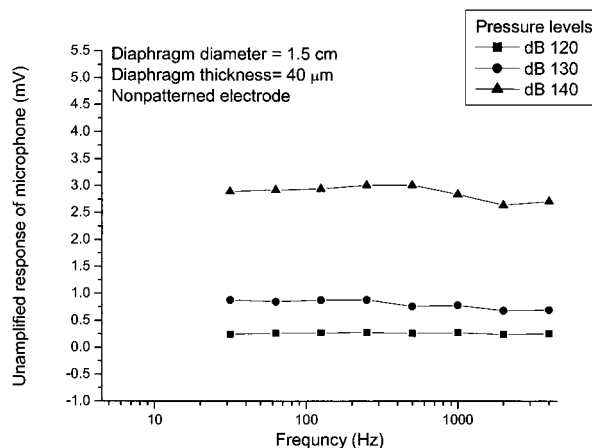


Fig. 6. Frequency response characteristic of acoustic sensor having diaphragm with nonpatterned electrode.

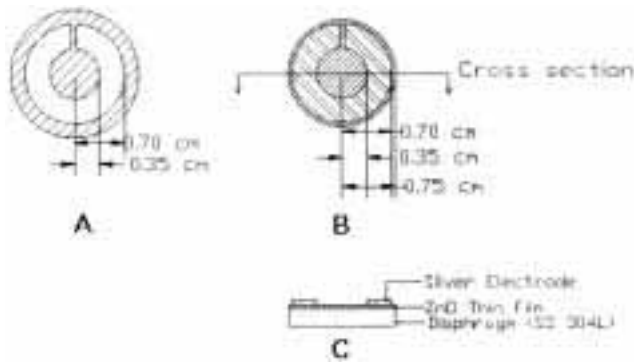


Fig. 7. (A) Schematic of mechanical mask used to obtain patterned electrodes on ZnO thin film. (B) Schematic of stainless-steel diaphragm with ZnO thin film and patterned silver electrodes onto ZnO thin film. (C) A cross-sectional view of diaphragm structure shown in (B).

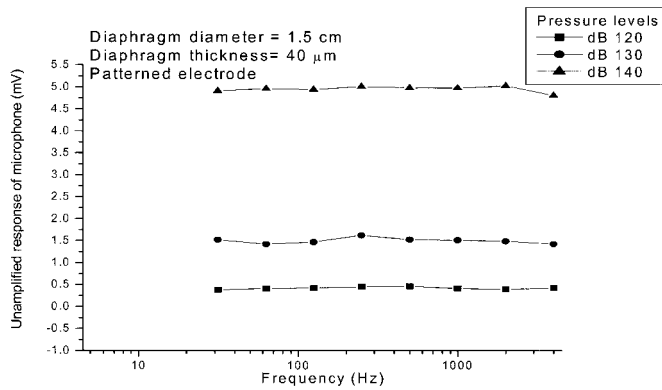


Fig. 8. Frequency response characteristic of acoustic sensor having diaphragm with patterned electrode.

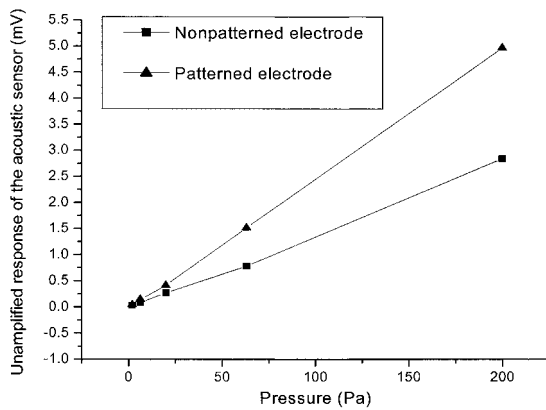


Fig. 9. Acoustic sensor output for patterned electrode as well as nonpatterned electrode for various pressures at 1 kHz.

sensors up to the limit of our testing apparatus (160 dB) for a forcing frequency of 1 kHz. It is evident from Fig. 9 that the acoustic sensor with patterned electrodes not only shows improvement in its output but also exhibits a linear response up to 150 dB.

#### 4. Conclusions

The output characteristics of a piezoelectric-thin-film-based acoustic sensor made with a stainless-steel diaphragm were studied. The details of the acoustic sensor diaphragm assembly, the deposition of the piezoelectric ZnO thin film, and the patterning of the electrode for enhancing the sensor out, among others were given. Note that the acoustic sensor developed exhibits a nearly flat frequency response and a linearity up to 150 dB (SPL). In comparison with conventional acoustic sensors, our acoustic sensor is attractive in view of its low cost, lower weight and simpler fabrication methods. Because of its low cost, it can be used as a disposable sensor in hazardous environments, under exposure to radiation, and in biomedical applications. It is also suitable for the measurement of high-intensity sounds.

#### References

- 1 M. L. Gayford: *Acoustical Techniques and Transducers* (MacDonald Evans Ltd., 1961).
- 2 H. F. Olson: *Elements of Acoustical Engineering* (Chapman and Hall Ltd., 1940).
- 3 S. Chowdhury, G. A. Jullien, M. A. Ahmadi and W. C. Miller: *Canadian Workshop on MEMS Micromachining: Applications, Devices and Technologies* (Ottawa, Canada, August 1, 1999).
- 4 D. P. Arnold, S. Gururaj, S. Bhardwaj, T. Nishida and M. Sheplak: *Proceedings of 2001 ASME International Mechanical Engineering Congress and Exposition* (New York, November 11–16, 2001).
- 5 C. H. Han and E. S. Kim: *MEMS* (2000) 148.
- 6 R. P. Ried, E. S. Kim, M. Hong and R. S. Muller: *J. MEMS* **2** (1993) 111.
- 7 S. S. Lee, R. P. Ried and R. M. White: *J. MEMS* **5** (1996) 238.
- 8 S. C. Ko, Y. C. Kim, S. S. Lee, S. H. Choi and S. R. Kim: *Sens. Actuators, A* **103** (2003) 130.
- 9 S. M. Sze: *Semiconductor Sensors* (John Wiley and Sons, New York, 1994).
- 10 F. S. Hickernell: *IEEE Ultrasonics Symposium* (1996) 235.
- 11 S. B. Krupanidhi and M. Sayer: *J. Appl. Phys.* **56** (1984).
- 12 F. S. Hickernell: *IEEE Transaction on Sonic and Ultrasonics* **SU-32** (1985) 621.
- 13 E. S. Kim, J. R. Kim and R. S. Muller: *TRANSDUCERS '91, IEEE International Conference on Sensors and Actuators* (1991), *Tech. Digest* 270–3.
- 14 [www.dpamicrophones.com/Images/DM665.pdf](http://www.dpamicrophones.com/Images/DM665.pdf)
- 15 <http://www.ndt.net/article/az/ae/sensorsensitivity.htm>
- 16 M. Sheplak, J. M. Seiner, K. S. Breuer and M. A. Schmidt: *37th AIAA Aerospace Sciences Meeting & Exhibit* (Reno, NV, January, 1999) *AIAA Paper* 99-0606.